Molecular Crystals and Liquid Crystals

ISSN: 1542-1406 (Print) 1563-5287 (Online) Journal homepage: http://www.tandfonline.com/loi/gmcl20

Investigation of the effect of aluminum doped zinc oxide (ZnO:Al) thin films by spray pyrolysis

Khalid Dakhsi, Bouchaib Hartiti, Samira Elfarrass, Hervé Tchognia, Mohamed Ebn Touhami & Philippe Thevenin

To cite this article: Khalid Dakhsi, Bouchaib Hartiti, Samira Elfarrass, Hervé Tchognia, Mohamed Ebn Touhami & Philippe Thevenin (2016) Investigation of the effect of aluminum doped zinc oxide (ZnO:Al) thin films by spray pyrolysis, Molecular Crystals and Liquid Crystals, 627:1, 133-140, DOI: 10.1080/15421406.2015.1137134

To link to this article: http://dx.doi.org/10.1080/15421406.2015.1137134

Published online: 13 May 2016.

MOL. CRYST. LIQ. CRYST.
2016, VOL. 627, 133–140
http://dx.doi.org/10.1080/15421406.2015.1137134

Taylor & Francis
Taylor & Francis Group

Investigation of the effect of aluminum doped zinc oxide (ZnO:Al) thin films by spray pyrolysis

Khalid Dakhsi[a], Bouchaib Hartiti[a], Samira Elfarrass[a], Hervé Tchognia[a], Mohamed Ebn Touhami[b], and Philippe Thevenin[c]

[a]Laboratory MAC & PM, team AN & PMAER, Departement of Physics, University Hassan II, FST Mohammedia, Maroc; [b]Laboratory LMEE, Faculty of science Kenitra, Kenitra, Maroc; [c]Laboratory LMOPS, University of Lorraine, Metz, France

ABSTRACT

In this study, aluminum doped zinc oxide thin films were deposited on ordinary glass substrates at the temperature of 425°C by spray pyrolysis technique for various doping concentrations of aluminum ranging from 1 to 5 at.%. The effect of dopant concentration on structural, morphological and optical properties of ZnO:Al thin films was studied. Optical band gap of the films increased with doping percentage and started to decrease from 2 at.% of dopant. The average transmittance for 2at.% ZnO:Al film is significantly increased over 90% in the visible region at 450 nm which is crucial for optoelectronic applications.

Introduction

In basic and technological research, a large number of transparent conducting oxides (TCO) such as ITO, SnO_2, In_2O_3, ZnO have been widely investigated [1–7]. Among these, Tin doped indium oxide (ITO) is the most widely used due to its low resistivity ($\sim 2\times10^{-4}\ \Omega\ Cm$) and its high transparency (~90%) at 550 nm [8–10]. However, the scarcity and therefore the high cost of indium make the ITO films very expensive. Recently, pure or doped zinc oxide is actively studied as an alternative to ITO material because of the non-toxicity and the availability of Zn element in the earth crust. In the last decade, zinc oxide thin film has attracted much attention due to its interesting properties such as high resistance to chemical attack, thermal stability, stability in hydrogen plasma commonly used in the fabrication of amorphous silicon solar cells, non toxicity and good adherence to many substrates. It is also a n-type semiconductor with a wide band gap (Eg = 3.3–3.4 eV), which has high optical transmission in the visible region [11–15]. In the case of wide band gap semiconductors, electrical conductivity is mainly due to the intrinsic defects such as interstitial zinc atoms and oxygen vacancies. thereby doping substantially changes their optical and electrical properties [16]. Usually in ZnO, the group III elements (like In, Al, Ga) or group VII elements (such as Fluorine) are used as dopants to produce samples having better electrical conductivity. Doping of ZnO results in the replacement of Zn^{2+} ions with the dopant atoms.

Many techniques have been previously used to deposit ZnO/ZnO:Al films on different substrates. These include filtered vacuum arc [16], sol–gel process [17], chemical spray pyrolysis

CONTACT Khalid Dakhsi dkhissi345@hotmail.com
Color versions of one or more of the figures in the article can be found online at www.tandfonline.com/gmcl.

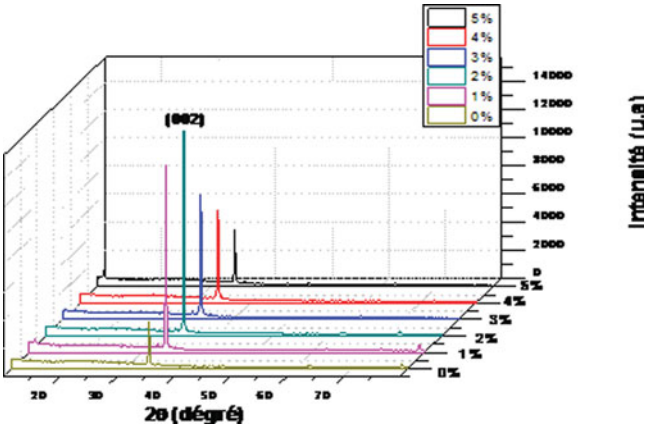

Figure 1. XRD patterns of ZnO and ZnO:Al fims with different doping concentration.

(CSP) [18], chemical vapor deposition (CVD) [19], pulsed laser deposition [20], molecular beam epitaxy (MBE) [21], electro-deposition[22], electron beam evaporation [23], chemical bath deposition (CBD) [24] and sputtering [25]. Of these, CSP technique is simple, low cost and can be used effectively for the deposition of large area thin films. In CSP, there is an easy control of roughness leading to light scattering which is a useful tool in solar cells and ease of tailoring of film properties for desired application by changing deposition and post deposition conditions. This work is aimed to prepare Al doped zinc oxide thin films by spray pyrolysis technique on ordinary glass substrates at 425°C and to analyze the effect of Al concentration on the structural, morphological, optical and electrical properties of ZnO thin films.

Experimental details

Undoped ZnO and aluminum doped ZnO thin films at different dopant percentages were deposited by CSP on ordinary glass substrates. This technique is most suitable for the deposition of oxide films. The deposition solution involved the decomposition of aqueous solution of 0.1 M zinc chloride ($ZnCl_2$). To achieve aluminum doping, aluminum nitrate ($Al(NO_3)_3$) was added to the solution. The doping percentage used in the starting solution in at.% were 1, 2, 3, 4 and 5. The resulting mixture was sprayed onto the preheated glass substrates held at the temperature of 425°C using compressed ambient air as carrier gas. Other parameters involved in all experiments (like spray rate: 1ml/min, nozzle to substrate distance: 30 Cm …) were kept constant.

The structural characterization of deposited thin films was carried out by analyzing the X-ray diffraction (XRD) patterns and surface morphology was studied using a scanning electron microscope (SEM). The resistivity of the film was calculated from the Four-point probe measurements. The transmission spectra were recorded at room temperature and near to the normal incidence using a Lambda 900 UV/VIS/NIR spectrometer.

Results and discussion

Structural analysis(XRD)

Figure 1 shows the x-ray diffraction patterns of ZnO:Al thin films with different Al concentration at the substrate temperature of 425°C. The position of the diffraction peaks observed

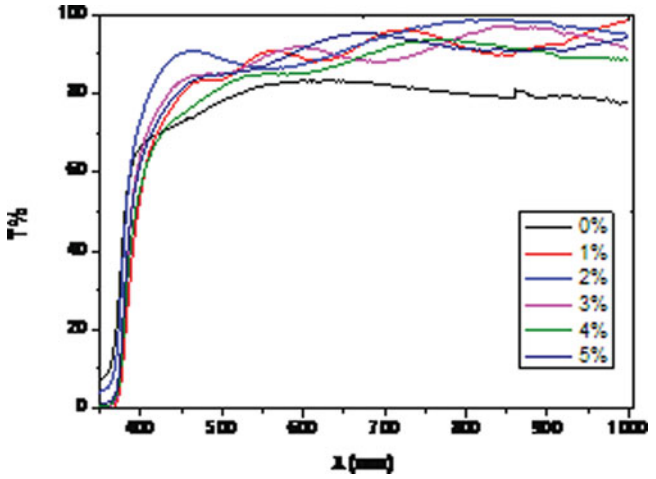

Figure 2. Transmittance spectra of films prepared at different atomic ratios of aluminum.

in all samples match well with those reported for ZnO wurzite structure [26]. The structure of all the films was polycrystalline and the results agree with that reported in [27]. It can be observed that in all ZnO:Al films, the most predominant peak is the (002) reflection indicating preferred orientation along the c-axis perpendicular to the substrate surface. No additional x-ray peaks are detected. However their relative intensities have a strong dependence on Al doping. The intensity of the (002) peak increases as the concentration of aluminum increases and starts decrease after 2 at.% of dopant due probably to segregation of Al_2O_3 into the grain boundaries [28] which inhibits the growth of the particle size in the films. That is one of reasons why the crystalline quality of films is found to deteriorate for Al concentration greater than 2 at.%. A similar behavior has also been reported in [29] and found that interstitial inclusion of dopant atoms deteriorate the film structure and lead to the undoped structure. Hence it is important to say that increasing the Al concentration in the solution increases the occupation of Al^{3+} in the interstitial position rather than the substitution of Zn^{2+} site which degrades the crystalline quality of the films for higher Al doping levels. The amount of doping modifies the film growth process. The decrease in the intensity of (002) preferential orientation for Al concentration greater than 2 at.% may also indicate a meaningful increase of staking defects and a loss of periodicity in the arrangement of ZnO crystals.

Optical properties

Transmittance and energy band gap

Figure 2 shows the optical transmission spectra of zinc oxide films deposited on ordinary glass substrate at the substrate temperature of 425°C for various aluminum doping concentrations. All films are highly transparent in the visible range (380–850 nm) of the optical spectrum reaching values up to 90% at 450 nm for 2 at.% of aluminum doping. We can also note that all obtained films could be used as optical windows in optoelectronic devices. According to theoretical and practical results, ZnO exhibits direct inter band transitions [30] and for allowed direct transitions between parabolic bands, the variation of absorption coefficient α with photon energy $h\nu$ obeys to the relation [32]:

$$(\alpha h\nu)^2 = A(h\nu - E_g)$$

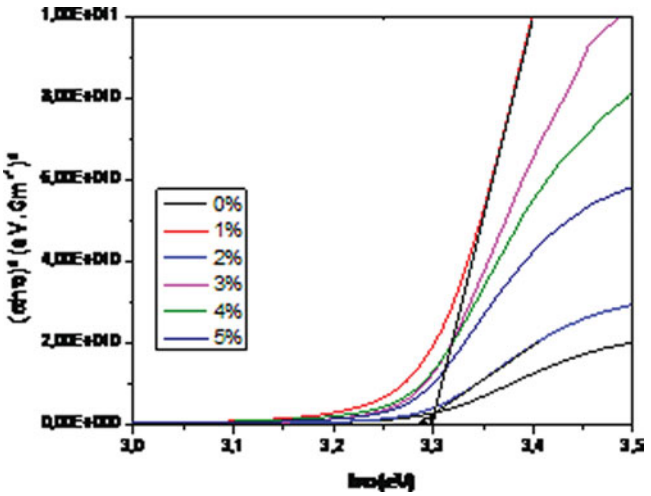

Figure 3. Plot of $(\alpha h\upsilon)^2 \upsilon s(h\upsilon)$ **for** films prepared at different aluminum doping concentrationFig. 4: Raman spectra of ZnO doped Al layers.

Where $h\upsilon$ is photon energy, α the absorption coefficient, A is a constant and E_g the band gap.

The plot of $(\alpha h\upsilon)^2 \upsilon s(h\upsilon)$ is shown in Fig. 3, the band gap value can be determined by extrapolating the linear part of the curve to the zero absorption ($\alpha = 0$) as indicated on the plot. It was observed that as the aluminum concentration increases, the absorption edge shifts in monotonously to a lower energy value from 3.29 eV to 3.37 eV for 0 at.% to 5 at.% respectively. This agrees with Ashour et al. [32] where they found optical gaps varying from 3.31 eV to 3.21 eV with increasing aluminum doping. This decrease in the band gap is possibly due to band distortions in the ZnO lattice following to the introduction of impurities (doping) and to the increase of free electrons concentration. This is eventually the result of the occupation interstitial sites by the dopant atoms because these latter represent the principal native donors in the films [33].

Raman spectrometry and photoluminescence

The structure of ZnO belongs to P63 mc space group. Group theory predicts the presence of two vibration modes A1, 2 E1 modes, 2 E2 modes and 2 B1 modes [34]. Among these modes, the modes A1 and E1 are polar and are divided into transverse optical phonons (OL) and longitudinal optical phonon (OL), all of which are active in Raman and infrared. E2 modes are only active Raman modes and B1 are neither active nor Raman active infrared; they are silent modes. A1 modes (OT), A1 (LO), E1 (EO), E1 (OL), E2 (bass) and E2 (high) are located at 376 cm^{-1} and 578 cm^{-1}, 418 cm^{-1} and 583 cm^{-1}, 101 cm^{-1} and 436 cm^{-1} [35].

Figure 4 shows the Raman spectra of ZnO thin films doped Al. In these spectra we can see specific vibration modes in ZnO. The ZnO nanoparticles show common patterns that are observed at 233, 290, 338 cm^{-1} (vibration second order corresponding to a combination of low and high frequency modes E2), 351 cm^{-1} (A1 (EO)), 438 cm^{-1} (high frequency E2), 574, 576, 580 cm^{-1} (E1 (OL) and 629 cm^{-1} (combination of E2 modes (bass) and B1 (high), respectively. The modes 233, 290 and 338 cm^{-1} could be observed by increased phonon Raman active and inactive with a symmetry of the network due to the disorder-activated Raman shift [36, 37]. Position 438 cm^{-1} is the ZnO wurtzite E2 mode and a very important feature. The E1 Mode

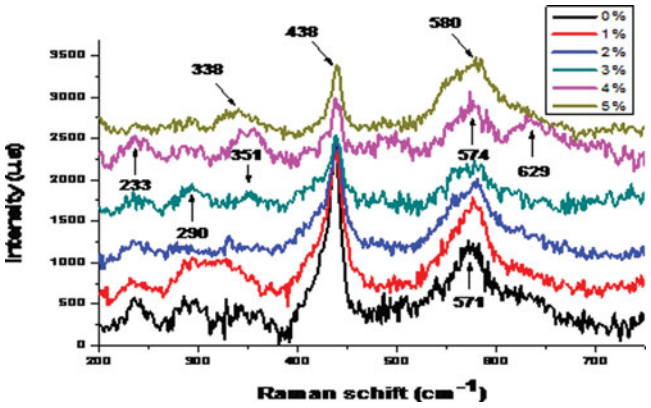

Figure 4. Raman spectra of ZnO doped Al layers.

(OL) at positions 574, 576 and 580 cm^{-1} corresponds to well resolved Raman peaks due to multiphonon process and resonance which relate to an oxygen deficiency [34, 36].

The first peak (a:ZnO pure and b: Al doped ZnO 1%) is centered at 376 nm, and corresponds to the transition of the optical gap of ZnO, or a gap of 3.31 eV which is in agreement with the values observed in the ZnO and which are around 370 – 372 nm [38]. As dopant is incorporated NBE emission peak shows blue-shift to 396 nm for samples c, e and f respectively.

The PL emission at 512 nm is the characteristic emission of ZnO thin films. This emission was extremely broad and this might be due to phonon-assisted transition [40]. But the exact reason for this emission is not clearly understood. Ratheesh Kumar et al. [39] concluded that this emission was due to the transition from conduction band to the acceptor level corresponding to the oxygen antisite (OZn). Interestingly the blue–green emission is not present in the case of samples doped process and it is this set of samples which exhibits the lowest resistivity after doping. the resistivity of the samples has strong correlation with intensity of the blue–green emission[41]. in our result it was observed that when the intensity of blue–green emission decreased, resistivity of the sample decreased[42].

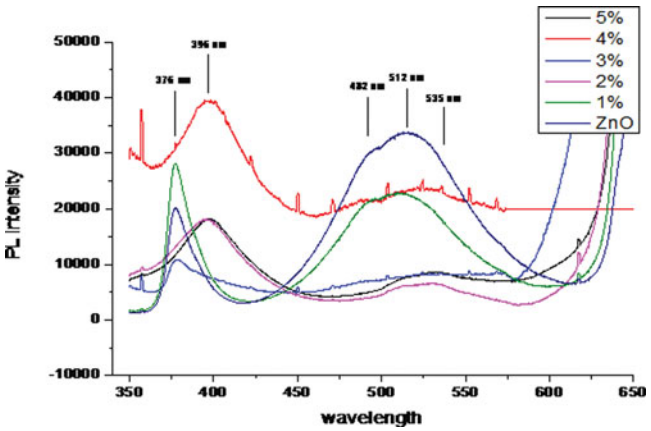

Figure 5. Photoluminescence of samples: a) ZnO pure, b) AZO 1%, c) AZO 2%, d) AZO 3% e) AZO4%, f) AZO 5%.

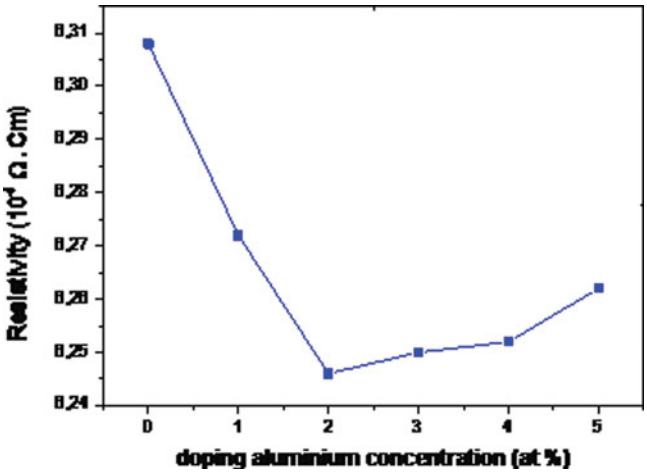

Figure 6. Variation of the resistivity as a function of Al doping concentration for Al doped ZnO films.

Electrical properties

Figure 6 is the plot of resistivity versus percentage of Al dopant. It can be observed that the resistivity decreased from 6.308×10^{-3} Ω *Cm* for undoped films to a minimum of 6.246×10^{-3} Ω *Cm* for films prepared with 2 at.% of dopant. The resistivity then started increasing with doping concentration to 6.262×10^{-3} Ω *Cm* at 5 at % doping. The decrease in the resistivity with increasing doping concentration is due to the increased number of free charge carriers (electrons) of Al^{3+} donors ions incorporated in interstitial sites of Zn^{2+} [43]. Small amounts of aluminum introduce large numbers of free electrons in the doped films and the conductivity therefore increases. But excess amounts of aluminum cannot be accommodated into ZnO lattice due to its limited solid solubility and therefore form neutral aluminum oxide (Al_2O_3) and segregates in the grain boundaries [44]. This is why further increase of aluminum concentration (>2 at.%) does not further increase the conductivity. Additionally, it has been shown that the electrical resistivity value of doped films is inversely proportional to the prevalence of the (002) orientation of film [45]. This mean more the peak intensity is sharp, the electrical resistivity is lower.

Conclusions

Al doped zinc oxide transparent films (ZnO:Al) were prepared by spray pyrolysis technique starting with zinc chloride and aluminum nitrate as sources of Zn and Al respectively. When the Al concentration increased from 0 at.% to 5 at.%, the films were oriented more preferentially along the (002) direction, the grain size of films increased, the transmittance also became higher and the electrical resistivity decreased. The optical band gap decreased with doping concentration from 3.29 eV to 3.27 eV for the doping concentration increasing from 0 at.% to 5 at.%. Films doped with 2 at.% Al had stronger orientation along the (002) direction, large grains, higher conductivity and transmittance than those of the other doped films. The properties of films produced at optimum conditions are suitable for optical and electrical applications owing to their low resistivity, higher optical transmittance in the visible region of the solar spectrum.

References

[1] Untila, G. G., Kost, T. N., & Chebotareva, A. B. (2009). *Thin solid films*, *518,* 1345–1349.
[2] Sung, Y.-M., & Han, D.-W. (2008). *Vacuum.*, *83,*161–165.
[3] Iwata, K., Sakemi, T., Yamada, A., Fons, P., Awai, K., Yamamoto, T., Shirakata, S., Matsubara, K., Tampo, H., Sakurai, K., Ishizuka, S., & Niki, S. (2005). *Thin solid films*, *480–481,* 199–203.
[4] Muller, J., Rech, B., Springer, J., & Milan, V. (2004). *Solar energy*, *77,* 917–930.
[5] Park, S.-M., Ikegami, T., Ebihara, K., & Shin, P.-K. (2006). *Appl. Surf. Sci.*, *253,* 1522–1527.
[6] Montero, J., Herrero, C., & Guillen, J. (2010). *Sol. Energy Mater. Sol. Cells*, *94,* 612–616.
[7] Huang, Y., Li, G., Feng, J., & Zhang, Q. (2010). *Thin solid films*, *518,* 1982–1896.
[8] Kim, H., Pique, A., Horwitz, J. S., Mattoussi, H., Murata, H., Kafafi, Z. H., & Chrisey, D. B. (1999). *Appl. Phys. Lett.*, *74,* 3444–3446.
[9] Qadri, S. B., Kim, H., Horwitz, J. S., & Chrisey, D. B. (2000). *J. Appl. Phys.*, *88,* 6564–6566.
[10] Kim, H., Horwitz, J. S., Kim, W. H., Makiinen, A. J., Kafafi, Z. H., & Chrisey, D. B. (2002). *Thin Solid Films*, *420–421,* 539–543.
[11] Krunks, M., Katerski, A., Dedova, T., OjaAcik, I., & Mere, A. (2008). *Sol. Energy Mater. Sol. Cells*, *92,* 1016–1019.
[12] Gledhill, S., Grimm, A., Allsop, N., Koehler, T., Camus, C., Lux-Steiner, M., & Fischer, C.-H. (2009). *Thin Solid Films*, *517,* 2309–2311.
[13] Wang, Z. A., Chu, J. B., Zhu, H. B., Sun, Z., Chen, Y. W., & Huang, S. M. (2009). *Solid State Electron.*, *53,* 1149–1153.
[14] Kashyout, A. B., Soliman, M. E., Gamal, E., & Fathy, M. (2005). *Mater. Chem. Phys.*, *90,* 230–233.
[15] Jeong, W. J., Kim, S. K., & Park, G. C. (2006). *Thin Solid Films*, *506–507,* 180–183.
[16] David, T., Goldsmith, S., & Boxman, R. L. (2004). *Thin Solid Films*, *447–448,* 61–67.
[17] Hong-ming, Z., Dan-qing, Y., Zhi-ming, Y., Lai-rong, X., & Jian, L. (2007). *Thin Solid Films*, *515,* 6909–6914.
[18] El Manouni, A., Manjon, F. J., Perales, M., Mollar, M., Mari, B., Lopez, M. C., & Barrado, J. R. (2007). *Superlattices Microstruct.*,, *42,* 134–139.
[19] Kim, D., Yun, I., & Kim, H. (2010). *Curr. Appl. Phys.*, doi:10.1016/j.cap.2010.02.030.
[20] Kim, H., Horwitz, J. S., Kim, W. H., Makinen, A. J., Kafafi, Z. H., & Chrisey, D. B. (2002). *Thin Solid Films*, *420–421,* 539–543.
[21] Nakahara, K., Takasu, H., Fons, P., Yamada, A., Iwata, K., Matsubara, K., Hunger, R., & Niki, S. (2002). *J. Cryst. Growth.*, *237–239,* 503–508.
[22] Wellings, J. S., Samantilleke, A. P., Warren, P., Heavens, S. N., & Dharmadasa, I. M. (2008). *Semicond. Sci. Technol.*, *23,* 125003–1250010.
[23] Sahu, D. R., Lin, S., & Huang, J. (2008). *Thin solid films*, *516,* 4728–4732.
[24] Shishiyanu, S. T., Lupan, O. I., Monaico, E. V., Ursaki, V. V., Shishiyanu, T. S., & Tiginyanu, I. M. (2005). *Thin Solid Films*, *488,* 15–19.
[25] Guillen, C., & Herrero, J. (2006). *Thin Solid Films*, *515,* (2) 640–643.
[26] *Powder Diffraction File, Data Card 5–644, 3c PDS.*, International Center for Diffraction Data, Swartmore, PA.
[27] Castaneda, L., Garcia-Valenzuela, A., Zironi, E.P., Canetas-Ortega, J., Terrones, M., & Maldonado, A. (2006). *Thin Solid Films*, *503,* 212.
[28] Majumder, S. B., Jain, M., Dobal, P. S., & Katiyar, R. S. (2003). *Mater. Sci. Eng. B.*, *103,* 16–25.
[29] Goyal, D., Solanki, P., Maraghe, B., Takwale, M., & Bhide, V. (1992). *Jpn. J. Appl. Phys.*, *31,* 361.
[30] Cetinorgu, E. & Goldsmith, S. (2007). *J. Phys. D: Appl. Phys.*, *40,* 5220–5236.
[31] Ohta, Y., Haga, Y., & Abe, Y. (1997). *Jpn. J. Appl. Phys.*, *36,* L1040–L1042.
[32] Ashour, A., Kaid, M. A., El-Sayed, N. Z., & Ibrahim, A. A. (2006). *Applied Surface Science*, *252,* 7844–7848.
[33] Pawar, B. N., Jadkar, S. R. & Takwal, M. G. (2007). *Solar Energy Materials & Solar Cell*, *91,* 258.
[34] Pal, U., Serrano, J. G., Santiago, P., Xiong, G., Ucer, K. B., & Williams, R. T. (2006). *Opt. Mater.*, *29,* 65–69.
[35] Ke, X., Shan, F., Shin Park, Y., Wang, Y., Wenzhe Fu, T., & Won Kang, D. (2007). *Surface and Coatings Technology*, *201*, 15, 6797–6799.
[36] Mead, D. G., & Wilkinson, G. R. (1977). *J. Raman Spectrosc.*, *6,* 123–129.

[37] Li, B. B., Xiu, X. Q., Zhang, R., Xie, Z. L., Chen, Y., Shi, Y., Han, P., & Zheng, Y. D. (2004). Semiconducting and Insulating Materials, SIMC-XIII 13 International conference 202–205.
[38] Ashkenov, N., Mbenkum, B. N., Bundesmann, C., Riede, V., Lorenz, M., Spemann, D., Kaidashev, E. M., Kasic, A., Schubert, M., & Grundmann, M. (2003). *Journal of Applied Physics*, *93,*126.
[39] Ratheesh Kumar, P. M., Sudha Kartha, C., Vijayakumar, K. P., Abe, T., Kashiwaba, Y., Singh, F., & Avasthi, D. K. (2005). *Semicond. Sci. Technol.*, *20,* 120–126.
[40] Reynolds, D. C., Look, D. C., Jogai, B., & Mokoc, H. (1997). *Solid State Commun.*, *101,* 643–646.
[41] Vimalkumar, T. V., Poornima, N., Sudha Kartha, C., & Vijayakumar, K. P. (2010). *Appl. Surf. Sci.*, *256,* 6025–6028.
[42] Vimalkumar, T. V., Poornima, N., Jinesh, K. B., Sudha Kartha, C., & Vijayakumar, K. P. (2011). *Applied Surface Science*, *257,* 8334–8340.
[43] Li, X. Y., Li, H. J., Wang, Z. J., Xia, H., Xiong, Z. Y., Wang, J. X., & Yang, B. C. (2009). *Optics Communications*, *282,* 247.
[44] Gomez-Pozos, H., Maldonado, A., & de la L. Olver, M. (2007). *Mater. Lett.*, *61,* 1460–1464.
[45] Lee, J.-H., & Park, B.-O. (2003). *Thin Solid Films*, *426,* 94.